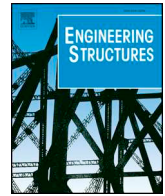




ELSEVIER

Contents lists available at ScienceDirect

Engineering Structures

journal homepage: www.elsevier.com/locate/engstruct

A unified macro-modelling approach for masonry-infilled RC frames strengthened with composite materials

D.A. Pohoryles*, D.A. Bournas

European Commission, Joint Research Centre (JRC), Ispra, Italy

ARTICLE INFO

Keywords:

Composites
Seismic retrofit
Infilled RC frames
Masonry infills
Macro-model

ABSTRACT

Non-structural masonry infills in existing reinforced concrete (RC) frame structures are known to affect their seismic behaviour significantly with potential detrimental effects. Increasing experimental evidence is available for the use of composite materials, such as fibre-reinforced polymers (FRP) and textile reinforced mortars (TRM), for in-plane retrofitting of brittle masonry infills. In order to apply such strengthening solutions in practice, adequate analytical models for predicting the behaviour are needed, however the large variation in infill properties already makes modelling the behaviour of non-retrofitted infills a challenge. Based on existing experimental and numerical studies on retrofitted infills, a macro-model is proposed, comprising a tie to account for the tensile strength of the composites materials, but also an increased compressive strut width due to the composite materials improving connection of the infill to the frame. After compiling a database of experimental data for composite retrofitted specimens tested in the literature, empirical equations for tie and strut strength was obtained. These equations constitute the first unified approach for FRP- and TRM-strengthened infills and were verified against the largest database of experimental results to date. The strut model was calibrated for the increase in strut width in terms of experimentally obtained stiffness increase, while the tie model was determined based on the remaining increase in strength. The empirical equations were shown to achieve a relatively high correlation with experimental results and to represent the mechanics of tested specimens well in terms of observed damage, hence indicating their potential for use as design-oriented equations for composite strengthened infills.

1. Introduction

The large proportion of existing reinforced concrete (RC) buildings built before the 1970's or 80's, hence before the introduction of modern guidelines that imposed more adequate seismic design of structures in Europe [1], puts the existing building stock in seismic countries at risk of significant economic losses, severe injuries and loss of human lives. In recent earthquakes, non-structural masonry infill walls have been the cause of unwanted brittle building failures, often altering the intended response of a structure [2–4]. Under in-plane loading, the presence of infill walls in RC frames generally leads to increased lateral resistance, enhanced stiffness, and hence a reduction in displacement demand on the frame [5–8]. Local failure of the infill panels due to in-plane mechanisms, but also out-of-plane collapse triggered by in-plane damage, may cause a sudden drop in capacity and hence brittle failure of the structure [9–13]. Infills are found responsible for high costs associated to losses even at low intensity earthquakes due to damage in non-structural infills [14]. These vulnerable structures require fast, reliable, and effective retrofit strategies. The need for increasing the rate of retrofitting ageing buildings has

also been recognised recently in the European Green Deal, which calls for a 'renovation wave' of the existing building stock [15].

Composite materials can achieve strengthening of the masonry infills and provide also adequate connection to the surrounding RC frame, leading to a reliable and ductile response of infilled RC frames by utilising the strength and stiffness of the masonry infills. For instance, fibre reinforced polymer (FRP) sheets have been applied as strips in the diagonal of the infill wall, leading to considerable strength increase [16–18]. This strength increase was however not found to be proportional to the strip width [19]. Strengthening by means of horizontal FRP strips, in turn, did not lead to significant increase in lateral capacity [20]. FRPs comprise a very popular strengthening material due to their high strength to weight ratio, small thickness increase and corrosion resistance. While high increases in strength and ductility can be achieved with FRPs [21,22], their application is also associated to some drawbacks, as the use of epoxy leads to higher costs and the need for the use of protective equipment.

Instead of using epoxy-based resin as binder, inorganic matrices (e.g. lime or cement-based mortars) can be combined with open-grid textile reinforcement (i.e. glass, basalt, carbon), leading to so-called textile

* Corresponding author.

E-mail addresses: Daniel.POHORYLES@ec.europa.eu (D.A. Pohoryles), Dionysios.BOURNAS@ec.europa.eu (D.A. Bournas).<https://doi.org/10.1016/j.engstruct.2020.111161>

Received 17 January 2020; Received in revised form 11 June 2020; Accepted 22 July 2020

Available online 21 August 2020

0141-0296/© 2020 The Authors. Published by Elsevier Ltd. This is an open access article under the CC BY license (<http://creativecommons.org/licenses/by/4.0/>).

reinforced mortar (TRM) composites [23,24]. The use of mortars eases the application of the strengthening and reduces its cost. Moreover, the advantages of TRM over FRP systems also comprise better fire resistance [25,26] and behaviour at high temperatures [27–30], better bond and strain compatibility with masonry, as well as their applicability at low temperatures or on wet surfaces. Koutas et al. [31] applied TRM jacketing for strengthening the masonry infills of a 2/3-scaled, three-storey RC frame. Soft-storey failure was avoided, which led to an enhanced deformation capacity and strength increase. Further tests on full-face application found high strength increase and enhanced deformation capacities [32], particularly when mechanical interlock between textile mesh and mortar was enhanced by means of braided textiles [33,34]. The use of TRM applied as diagonal strips was found to be very effective, but the increase in width of the diagonal TRM layers was not found to significantly affect this strength increase [35]. TRM strengthening was also found to improve the interaction of in- and out-of-plane mechanism in masonry infilled RC frames, with reduction in in-plane damage found to improve the out-of-plane residual capacity [36–38]. Recently, the use of TRM has been successfully demonstrated for the out-of-plane strengthening [39], of masonry-infilled RC frames, but also offered alternatives for the concurrent seismic and energy retrofitting of RC and masonry building envelopes [39–42].

Despite increasing experimental evidence, simplified modelling is still needed to facilitate the use of TRM and FRP for strengthening masonry-infilled RC frames. Macro-models using compressive struts are commonly used for simplified modelling of infilled frames [43], and the aim of this paper is to propose a unified macro-modelling approach for composite strengthened infilled frames. An overview of existing macro-models for modelling composite-strengthened infilled frames is presented first; then the definitions for a proposed strut and tie model are presented. A database including all test results is developed, allowing for a sensitivity analysis on the parameters affecting the strengthening effectiveness.

This paper develops a new macro-model for masonry-infilled RC frames strengthened with composites. The presented model expands on the state-of-the-art, by proposing empirical equations for increased a compressive strut width together with the addition of a tensile tie, expressed with empirical equations calibrated against 26 experimental tests. The proposed equations constitute the first unified approach for FRP and TRM strengthened infills and are verified against the largest database of experimental results to date. A design safety factor and a design flow-chart are provided, highlighting the required parameters and the use of the developed equations. The development of these empirical equations for the strength and stiffness increase can hence be seen as an early attempt for design-oriented equations for strut-and-tie models for composite-strengthened infills, which may ease the implementation of said retrofit schemes in the field.

2. Existing modelling approaches

In this section the state-of-the-art on the simplified macro-modelling of composite-strengthened infilled RC frames is presented. While an increasing number of researchers have published experimental evidence highlighting the potential of using composite materials for strengthening masonry-infilled RC frames, reliable analytical models are needed to ensure a wider use of such retrofit methods. Modelling of masonry infills and their interaction with RC frames is a complex, but widely studied topic. The addition of composite materials as retrofit material adds further complexity to the problem. Advanced nonlinear finite element models of retrofitted infilled RC frames may be able to produce accurate results [e.g.: 44], their computational cost is however prohibitive for the seismic assessment of real buildings at scale and too complex for design-applications. Instead, a macro-modelling approach could be an adequate tool for retrofit design and assessment purposes, if reliable results can be obtained.

Macro-modelling of infilled frames is well-studied and exhaustive review papers on compressive strut-models can be found [43,45–50]. The principle of strut-models is that compressive strain is developed in the diagonal of the infill due to the flexural deformation of the surrounding RC

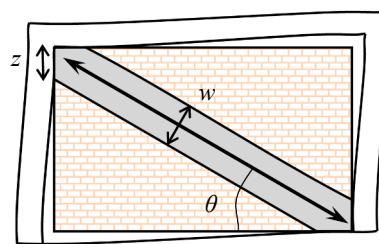


Fig. 1. Diagonal compressive-strut model for infilled frames.

members when increasing in-plane displacements are applied to the frame [51]. This forms the basis for the diagonal strut approach shown in Fig. 1.

After infill-frame separation, the contact between panel and frame is reduced to a contact length, z , giving rise to an effective compressive strut width, w , which defines the area of masonry involved in the lateral resistance. The degree of connectivity between the frame and the infill influences the width of the diagonal compressive strut which is assumed to resist the frame deformation under seismic loading [52]. If the infill is well-connected to the frame, a larger portion of the infill resists this deformation. In the case of poor connection, compressive forces are resisted by a thinner infill strut. This leads to a more localised stress concentration and hence early masonry failure.

To model infills retrofitted with composite materials, a macro-modelling approach combining the compression strut with tie elements taking tensile forces can be used. This may lead to a design-oriented tool for infill-retrofitting. The concept of combining a pair of diagonal macro-elements, with a single strut for compressive forces and a single tie for tensile forces, was first introduced by Binici et al. [53,54] for FRP-strengthened infills. The proposed model provided adequate results in push-over analyses, as it was shown to accurately estimate stiffness, strength and deformation capacity for a limited number of tested frames. Akin et al. [55] tested this strut-and-tie model by Binici et al. [53] for experimental results on three two-storey FRP-retrofitted infilled RC frames. The strength of the tie was defined based on the force resisted by the FRP reaching an effective strain of 0.2% in the infill diagonal. The compressive strut parameters were however assumed not to be affected by the FRP. The maximum strength of the experiments was well predicted by the model, with analytical results lying within 15% difference. The stiffness of the frames was however heavily underestimated, with differences up to 70% between the model and the experiments. Erol and Karadogan [16] also used a strut and tie macro-modelling approach for modelling CFRP strengthened infills. Again, the compressive strut was assumed not to be altered by the retrofit. The tensile tie force was based on a maximum FRP strain of 0.3% in the diagonal. The experiment results were well-matched by the analytical model in terms of maximum strength.

A strut-and-tie model was also used by Koutas et al. [56] to reproduce their experimental results on an infilled three-storey RC frame strengthened with TRM [24]. The effect of the TRM-retrofit was included in the definition of the tie properties by evaluating the tensile force in the retrofit material in the diagonal of the infill, assuming a multilinear crack pattern. Again, effective strain in the tie, ϵ_{te} , was found to be the main parameter affecting the model, with an estimation of 0.8% for the single layer of TRM and 0.57% for the double-layer, respectively found to match the results of the single experiment. To define the stiffness of the tie, an effective tie length, accounting for the crack distribution along the diagonal is used. Values between 0.11 and 0.5 of the diagonal length were found to have limited effect on the model, with a suggested value of 0.25. Recently, a calibration study for a database of TRM-strengthened specimens has offered an empirical equation for effective strain used to modify this model [57].

In terms of the compressive strut, material characterisation tests on masonry wallets strengthened with composites have shown that while the cracking stiffness is enhanced significantly, the vertical compressive material properties of the retrofitted infill itself are not altered considerably by the retrofit [e.g.: 54]. The compressive strut may however still be affected by the composite retrofitted as hypothesised by

Breveglieri et al. [44], who proposed an increase in strut width, w , due to FRP-strengthening of the masonry-infill panels. This increase may be associated to the better connection of the infill to the frame, as well as the enhanced confinement of the masonry elements. By means of a finite-element model (FEM) calibrated on experimental results, a correction factor, Ω_s , for strut width increase was proposed in [44] for FRP-strengthened infills and is defined based on the reinforcement ratio of FRP in the plane of the strut, ρ_f in Eq. (1):

$$\Omega_s = 0.24 \cdot \ln \rho_f + 2.67 (R^2 = 0.86) \quad (1)$$

where the FRP reinforcement ratio is given by the fraction of FRP area, A_f , projected from the angle of the tie, θ , onto the axis of the vertical, over the area of masonry infill ($h_w \cdot l_w$) in Eq. (2):

$$\rho_f = \frac{A_f \cdot \cos \theta}{h_w \cdot l_w} (\text{in}\%) \quad (2)$$

This coefficient has been calibrated by Breveglieri et al. [44] based on their parametric FE-study for an infilled frame strengthened with FRP strips of varying thickness and width. As can be seen, the coefficient of determination, R^2 , is close to 1, indicating an adequate goodness-of-fit.

In conclusion, based on the available literature, the effectiveness of the composite retrofit for masonry-infilled RC frames may be characterised by an increase in strength due to two mechanisms. On the one hand, the strengthening is characterised by the addition of a tensile tie compared to a sole strut-model for unreinforced masonry infills. This tie adds to the capacity of the infill by bridging the cracks in the masonry. In the models provided in the literature, this tie is usually calibrated based on very limited experimental data, giving one fixed value of tensile strain to calculate the tie force. On the other hand, also the compressive strut properties are enhanced by the retrofit, as the composite material improves the connection of the infill to the frame, hence activating a wider compressive strut. A limitation of most models to date, is that this effect is not considered, apart from the model by

Breveglieri [44], which however uses only one configuration and is calibrated on results from finite element modelling.

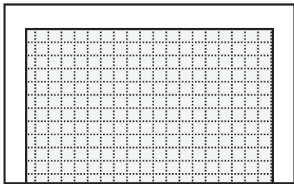
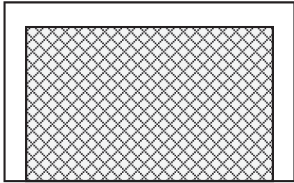
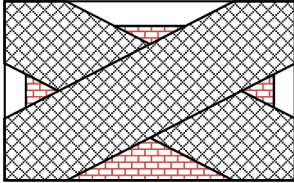
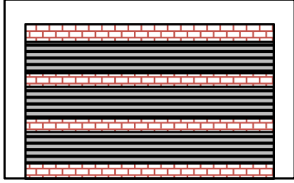
3. Proposed strut and tie definition for retrofitted infills

This section describes the proposed strut and tie modelling approach for composite-strengthened infills taken in this study. As shown in the previous section, the existing models proposed in the literature are only compatible for the specific method of strengthening evaluated and are usually based on a single experiment and typically add only a tensile tie without adapting the strut width. In order to achieve a unified macro-model for masonry infills strengthened with composite materials, it is proposed to define a model that includes not only a diagonal tie resisting a diagonal cracking pattern across the infill, but also an increase in strut-width due to enhanced infill-to-frame connection. The latter has so far only been considered using FEM-derived data by Breveglieri [44]. The proposed model will however be calibrated for a larger data set, using all available experimental results.

As can be seen in Table 1, geometrical parameters for different retrofit methods are diverse, with application of the composite over the full surface of the infill or as strips and different orientations of the fibres or meshes. To achieve a unified macro-model, that encompasses different materials and layouts of retrofit application, a reinforcement ratio compatible for the different types of composite retrofit, the effective geometrical ratio of composite reinforcement, ρ_{eff} , is first needed to be defined. This is similar to the ratio defined in Eq. (2) for FRP strips applied in the diagonal of the frame, but accounts for application of the composite in other angles than the diagonal, as well as composites that are not applied as strips.

As shown in Fig. 2, an effective width, $w_{eff,\theta}$, of activated material in diagonal tension is first defined. The angle α is defined as the angle of the composite applied, with directions i accounting for uni- or bi-directional materials. The use of an effective tie-width is analogous to the effective strut-width defined for macro-models of infills in compression

Table 1
Summary of masonry-infilled RC frames strengthened with composite materials in the literature.

Type	Layout	Strengthening material	Fibre direction	Examples
Orthogonal TRM		Fibre-textile	2	[31,32,34,36,37]
TRM at 45°		Fibre-textile	2	[36]
Diagonal TRM/FRP strips		Fibre-textile or Fibre-sheet	2 or 1	[16–19,35]
Horizontal FRP strips		Fibre-sheet	1	[20]

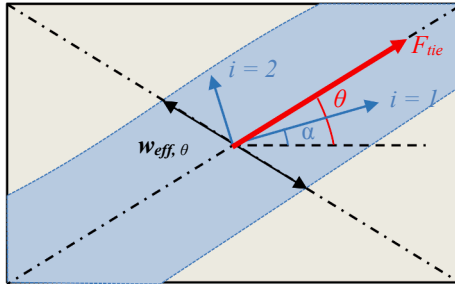


Fig. 2. Definition of local axes for the proposed diagonal tie model.

[58]. It considers that only a part of the area of the composite is involved in resisting the diagonal tension developed under horizontal loading, as cracking is not extended along the entire length of the tie diagonal. Note that for specimens in which the retrofit is applied as diagonal strips thinner than $w_{eff,\theta}$, the actual width of the strip is used.

This follows a similar logic to the concept of effective tie length used to define the stiffness of ties in previous macro-models. Here, the concept of effective tie width is used instead, as it affects the tie strength in an analogous way to the strut width. With the limited amount of experimental evidence, it is difficult to determine a precise value or equation for $w_{eff,\theta}$. Breveglieri et al. [44] considered half of the diagonal length (d_m), while Koutas et al. [56] found that varying between 0.11 and $0.5 \cdot d_m$ has limited effect and suggested a value of $0.25 \cdot d_m$. In terms of experimental evidence, Ismail et al. [35] tested the effect of three different TRM widths in the diagonal (1/6, 1/3 and full area) and found that the strength increase between them is relatively limited, particularly for stiffer carbon textile. Likewise, Altin et al. [19] found that an increase in diagonal FRP strip width between 0.13 and 0.27 of the diagonal width does not lead to a proportional strength increase, with limited strength increase for the wider strips.

In this study the value of $0.25 \cdot d_m$ is initially used as maximum effective width, however an empirical assessment and verification of the selected value is provided in Section 4.

$$w_{eff,\theta} = 0.25 \cdot d_m \quad (3)$$

The effective area of the tie is then evaluated based on the nominal thickness, t_{nom} , of the strengthening material and an effective width, $w_{eff,i}$, in each direction i . For bi-directional composites the effective width then needs to be transformed into the two directions of the mesh.

$$w_{eff,1} = \cos(\theta - \alpha) \cdot w_{eff,\theta} \quad (4)$$

$$w_{eff,2} = \sin(\theta - \alpha) \cdot w_{eff,\theta} \quad (5)$$

The nominal thickness, t_{nom} calculation is based on the nominal or equivalent thickness of the sheet or textile, which can be calculated based on the weight and fibre density [24]:

$$t_{nom} = \frac{a \cdot W}{\rho_{fibre}} \quad (6)$$

where a represents the fraction of the fibres in the respective direction ($a = 1$ for FRP and $a = 0.5$ for TRM with equal fibre distribution in the two directions, or according to the actual fibre distribution), W stands for the weight per m^2 and ρ_{fibre} is the fibre density per m^3 . The total effective area in the direction of the diagonal is then given by Eq. (7):

$$A_{eff} = n_s \cdot n_l \cdot t_{nom} \cdot w_{eff,\theta} \cdot [\cos(\theta - \alpha) + \sin(\theta - \alpha)] \quad (7)$$

where n_s is the number of retrofitted sides (1 or 2) and n_l the number of applied layers per side. The effective geometrical ratio can then be expressed according to equation

$$\rho_{eff} = \frac{A_{eff} \cdot \cos\theta}{h_w \cdot l_w} \quad (8)$$

Note that in the case of diagonal FRP application the sin term in Eq. (7) cancels out so that the same result as Eq. (2) is obtained.

From the effective geometrical ratio, the mechanical reinforcement ω_{eff} , is defined in Eq. (9), which also includes the ratio of the ultimate strength of the retrofit material, f_{fu} , and the compressive strength of the infill wall $f_{m,inf}$:

$$\omega_{eff} = \rho_{eff} \cdot \frac{f_{fu}}{f_{m,inf}} \quad (9)$$

3.1. Compressive strut definition

A number of analytical expressions exist for the definition of the strut parameters for macro-modelling masonry infills [e.g.: 58–61]. The empirical Eq. (10) for the equivalent strut width (w) by Mainstone [58,62] is widely accepted [e.g.: 45,48,63] and is also used here:

$$w = 0.56(\lambda \cdot H)^{-0.875} \cdot d_m [m] \quad (10)$$

H is the height of the frame, d_m the length of the diagonal, and λ represents the relative panel-to-frame stiffness defined by Eq. (11) by Stafford Smith and Carter [60]:

$$\lambda = \sqrt[4]{\frac{E_m \cdot t_{inf} \cdot \sin 2\theta}{4 \cdot E_c \cdot I \cdot h_w}} [m^{-1}] \quad (11)$$

With E_m and E_c , the elastic moduli of the masonry infill and the concrete framing members, respectively, t_{inf} the wall thickness, h_w is the infill wall height, I the second moment of area of the column. Note that according to ACI 530-11 [64] $E_m = 700 \cdot f_{m,inf}$ if an experimental value is unavailable. The strut force is then defined as the product of the maximum compressive infill strength in the direction of the strut, $f_{m,\theta}$, and the strut area ($w \cdot t_{inf}$). A commonly adopted empirical equation for the former is defined by Decanini et al. [65] in Eq. (12):

$$f_{m\theta} = \frac{1.12 \cdot f_{m,inf} \cdot \sin\theta \cdot \cos\theta}{K1 \cdot (\lambda \cdot H)^{-0.12} + K2 \cdot (\lambda \cdot H)^{0.88}} [MPa] \quad (12)$$

Such an approach is compatible with the chosen strut width definition and uses empirical parameters $K1$ and $K2$ defined based on the values of λ [65].

Again based on the strut width, the secant stiffness, K_m , of the infill is calculated using Eq. (13):

$$K_m = \frac{E_m \cdot t_{inf} \cdot w}{d_m} \cdot \cos^2\theta [kN/mm] \quad (13)$$

The increase in strut width due to the composite retrofit, hence affects the strut force and strut stiffness. Under the assumptions of the equations used for the strut and tie model, the increase in secant stiffness is only affected by the increase in strut width. To define the non-dimensional strut width increase factor Ω_s , the data from Breveglieri et al. [44] is used for comparison. However, the original Eq. (1) is modified, as the logarithmic definition leads to negative values at near-zero effective geometrical ratios ρ_{eff} . Instead the fitting curve is adapted to render a value of $\Omega_s = 1$ when no retrofit is applied ($\rho_{eff} = 0$). Moreover, the modified equation uses the mechanical reinforcement ω_{eff} , still keeping the non-dimensionality of Ω_s .

$$\Omega_{s,mod} = 0.14 \cdot \omega_{eff}^{0.57} + 1 (R^2 = 0.90) \quad (14)$$

As shown in Fig. 3, the proposed equation matches the data from finite-element modelling well and actually presents a similar goodness of fit (R^2 -value) to the original Eq. (1).

As the increase in secant stiffness, defined in Eq. (13), is directly proportional to the increase in strut width, the modified fit equation for Ω_s will be assessed by comparing it to the increase in stiffness obtained experimentally for all the experimental specimens available in the literature. Using the experimental data, a new empirical equation will be proposed based on the increase in secant stiffness.

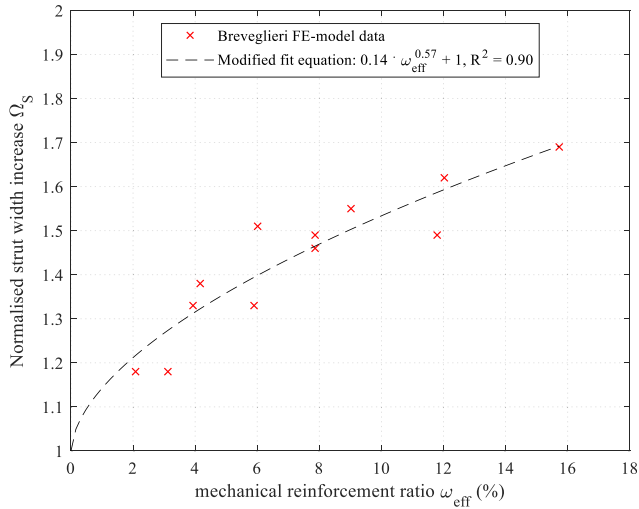


Fig. 3. Modified fit equation for strut width increase due to composite retrofitting.

3.2. Tensile tie contribution

The tensile tie contribution is finally determined based on the experimentally obtained strength increase between the retrofitted specimens and their respective control ones. This approach, shown in Fig. 4, is based on maximum obtained base shear and is similar to other studies evaluating macro-models for retrofitted infilled frames [e.g.: 16,19]. Assuming the RC frame itself is unchanged, the difference in capacity between retrofitted and control (non-retrofitted) specimens ($\Delta V_{exp} = V_{ret} - V_{con}$), can be defined as the sum of the increased compressive strut force, ΔV_{strut} , due to the increased strut width by the new Ω_s factor and the tensile force in the tie at the peak force, V_{tie} . Hence, $\Delta V_{exp} = V_{tie} + \Delta V_{strut}$.

Due to the variety of specimens in the experimental database, it is useful to also define the tie strength in terms of a strength increase due to the tie contribution (Ω_{tie}) normalised by the compressive strut force of the unretrofitted infill wall ($V_{strut,c}$) according to Eq. (15), which is analogous to the definition of the increase in strut capacity, Ω_s :

$$\Omega_{tie} = \frac{V_{tie}}{V_{strut,c}} \tag{15}$$

The above assumption clearly depends on the obtained failure mode in the experiments, most crucially, none of the specimens chosen failed due to a failure of the RC frame. A check of the obtained strain in the composite material is later performed (see Section 5.1), to ensure that the tie force is below the force corresponding to its fracture.

4. Calibration of empirical modelling equations

This section presents the calibration of the empirical equations for the proposed strut and tie model based on an experimental database of available studies on TRM and FRP retrofitted infills.

4.1. Experimental database

To derive an empirical equation to be used with the proposed unified macro-model for composite retrofits, experimental data from the literature was gathered for masonry-infilled frames strengthened with textile reinforced mortars (TRM), as well as fibre-reinforced polymers (FRP). Table 2 summarises the parameters and experimental results for 26 masonry-infilled RC frame specimens retrofitted with composite materials tested in the literature. Note that only frame specimens with a strong frame-weak infill configuration tested under cyclic loading are chosen, as well as specimens with an observed increase in strength and stiffness. Instead of using orthogonal textile meshes, the use of steel grids embedded in a thin layer of plaster for strengthening infills (reinforced plasters) is an alternative strengthening method [66,67], however it will not be considered here-in due to the plastic behaviour of the steel reinforcement.

Next to parameters of the tested infilled frames, including their scale, the angle of the diagonal (θ), the infill wall thickness (t_{inf}) and the infill wall compressive strength ($f_{m,inf}$), also the retrofitting characteristics, including the material (glass, carbon, basalt), composite type (TRM, FRP), the fibres ultimate strength (f_{fu}), the effective geometrical ratio of composite reinforcement (ρ_{eff}), as defined in Eq. (8), and the presence of anchorage (steel ties or bolts, fibre anchors) or not. The latter serves for completeness, is however not taken into account for the definition of the empirical equations. From the experimental results, the experimental base shear capacity percentage increase (ΔV_{exp}) and the

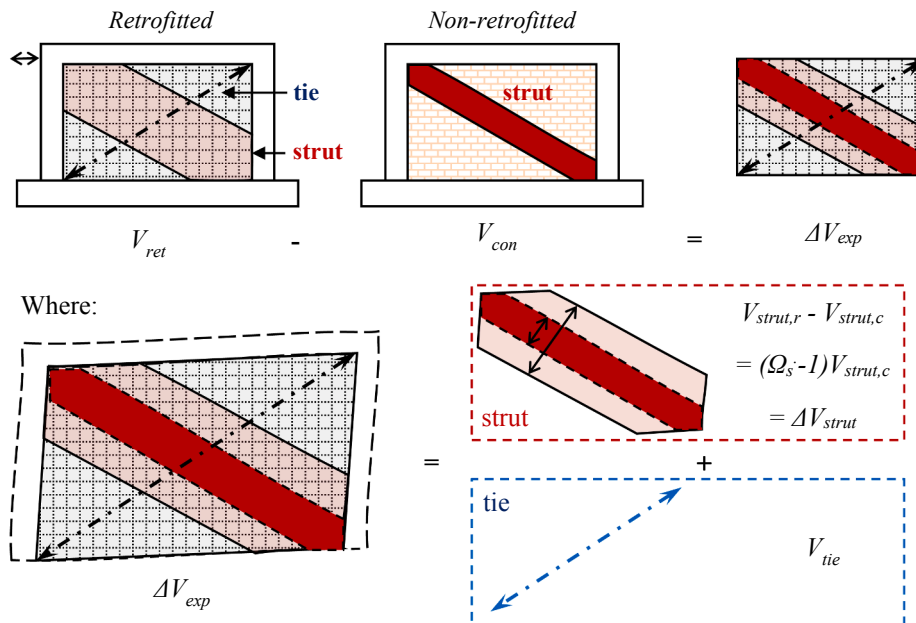


Fig. 4. A simplified approach for determining the tie strength at peak load.

Table 2
Composite strengthened infilled RC frame specimens tested in the literature.

Specimen	Scale	θ °	t_{inf} mm	$f_{m,inf}$ MPa	Material	f_f MPa	n_s	ρ_{eff} ‰	anch.	ΔV_{exp} %	ΔK_{exp} %	
Koutas-TRM	2/3	36	110	5.7	G	TRM	1825	2	0.065	fibre	54%	19%
Selim-SRG-2-2-A	1/3	41	75	2.5	G	TRM	1276	2	0.063	fibre	66%	11%
Akhoundi-CTRM	1/2	36	140	1.4	G	TRM	1296	2	0.013	fibre	25%	127%
Akhoundi-BTRM	1/2	36	140	1.4	G	TRM	1296	2	0.013	fibre	30%	127%
Ismail-RFG-D6-4	2/3	36	150	2.1	G	TRM	800	2	0.018	no	32%	23%
Ismail-RFC-D3-5	2/3	36	150	2.1	C	TRM	5040	2	0.029	no	40%	31%
Ismail-RFB-D3-7	2/3	36	150	2.1	B	TRM	1602	2	0.023	no	73%	21%
Ismail-RFB-D6-8	2/3	36	150	2.1	B	TRM	1602	2	0.016	no	99%	40%
Ismail-RFB-Fu-9	2/3	36	150	2.1	B	TRM	1602	2	0.033	no	54%	8%
Sagar-DU0-90	1/2	29	76	8.1	G	TRM	722	1	0.026	no	25%	29%
Sagar-DA0-90	1/2	29	76	8.1	G	TRM	722	1	0.026	steel	15%	28%
Sagar-SU0-90	1/2	29	76	8.1	G	TRM	722	1	0.026	no	11%	39%
Sagar-SA0-90	1/2	29	76	8.1	G	TRM	722	1	0.026	steel	30%	15%
Sagar-DA45	1/2	29	76	8.1	G	TRM	722	1	0.013	steel	29%	36%
Altin-FRP2	1/3	31	80	1.9	C	FRP	4100	2	0.044	fibre	118%	91%
Altin-FRP3	1/3	31	80	1.9	C	FRP	4100	2	0.066	fibre	144%	53%
Altin-FRP4	1/3	31	80	1.9	C	FRP	4100	2	0.080	fibre	162%	60%
Altin-FRP5	1/3	31	80	1.9	C	FRP	4100	1	0.022	fibre	58%	43%
Altin-FRP6	1/3	31	80	1.9	C	FRP	4100	1	0.033	fibre	79%	79%
Altin-FRP7	1/3	31	80	1.9	C	FRP	4100	1	0.040	fibre	84%	50%
Altin-FRP8	1/3	31	80	1.9	C	FRP	4100	1	0.022	fibre	54%	54%
Altin-FRP9	1/3	31	80	1.9	C	FRP	4100	1	0.033	fibre	71%	64%
Altin-FRP10	1/3	31	80	1.9	C	FRP	4100	1	0.040	fibre	86%	60%
Erol-N2	1/2	35	135	1.0	C	FRP	4300	2	0.031	fibre	44%	65%
Yuksel-CB	1/3	44	88	5.5	C	FRP	3900	2	0.022	fibre	21%	21%
Yuksel-CDB	1/3	44	88	5.5	C	FRP	3900	2	0.022	fibre	61%	61%

Note: material: G: glass; C: carbon; B: basalt.

Table 3
Correlation between experimental parameters and the normalised tie strength.

Parameter	θ	$\theta-\alpha$	$\rho_{f,eff}$	f_{fu}	$f_{m,inf}$	ω_{eff}
r -value (V_{tie})	-0.34	-0.37	0.70	0.49	-0.39	0.83
r -value (ΔK_m)	-0.08	0.04	-0.10	0.21	-0.43	0.52

increase in secant stiffness, i.e. the stiffness defined by the displacement at the maximum lateral loading obtained experimentally, compared to the as-built control specimen (ΔK_{exp}). Other parameters of interest may be the presence of openings in the infills or the presence of a cavity between multiple leaves of an infill wall, however no retrofitted specimens with such properties have been tested in the literature. The lack of such experimental data hence means that the model is limited to specimens without openings and or cavity.

4.2. Correlation between experimental and modelling parameters

By using the modified increase in strut width from Eq. (14), the strength increase due to the tie (Ω_{tie}) can be evaluated for all the specimens. With the range of parameters involved in the experiments, a more in-depth analysis by means of a statistical correlation test is first conducted. This allows to adequately assess the effect of individual parameters on the normalised tie strength and stiffness of retrofitted frames. The correlation with different experimental parameters is evaluated by conducting a statistical analysis, namely by calculating the correlation coefficient r . Positive correlation indicates that an increase in one parameter leads to an increase in the other, while a negative correlation means that an increase in one leads to a decrease in the other. The larger the r -value, the stronger the effect, with an r -value of ± 1 corresponding to perfect correlation. The r -values between various geometric and material parameters with the initially calculated tie strength, associated to Ω_{tie} , and the secant stiffness increase, associated to Ω_s , are shown in Table 3.

The angle of the diagonal, θ , and hence the aspect ratio of the tested frames appears to influence the tie strength with a low to moderate

negative correlation coefficient. When taking the difference between the diagonal angle and the angle of the strengthening material, similar correlation is obtained, indicating that an alignment of the fibres or grid with the diagonal ($\theta-\alpha = 0$) may achieve higher levels of normalised tie force, which is in line with observations from experiments. For the stiffness of the retrofitted fibres, no correlation with these two parameters is obtained instead.

Looking at the results in Table 3, a strong positive correlation for the tie strength is obtained with the effective geometrical ($\rho_{f,eff}$) of composite reinforcement. This, in turn, has a near-zero correlation with the increase in stiffness. A low-moderate positive correlation is obtained with the strength of the retrofit material, f_{fu} , for the increase in stiffness, but this is significantly more pronounced for the tie strength. Finally, another important aspect is the effect of the infill wall strength, $f_{m,inf}$, which negatively affects the tie strength and stiffness increase, as a moderate negative correlation is obtained. This for instance indicates that for stiffer infills the effectiveness of the retrofit in terms of strength increase is lower.

For both the tie strength and the increase in stiffness, the largest correlation coefficients are obtained for the combination of the individual parameters into a mechanical ratio of composite retrofitting material (ω_{eff}). This highlights the adequacy of its definition according to Eq. (9) and the proposed empirical models are hence defined in terms of ω_{eff} .

4.3. Increase in strut width

The increase in strut width due to composite retrofitting of the infilled RC frame is defined from the ratio of the experimentally obtained secant stiffness of retrofitted specimens to the secant stiffness of the non-retrofitted control specimens. It is plotted against the mechanical reinforcement ratio in Fig. 5. As mentioned previously, the secant stiffness increase is equivalent to the increase in strut width, if all other parameters in Eq. (13) remain unchanged between the retrofitted and control specimen. The modified Breveglieri equation for Ω_s (14) is compared to the experimental data and the data obtained from FE-modelling in [44]. As can be seen, the modified Breveglieri equation fits

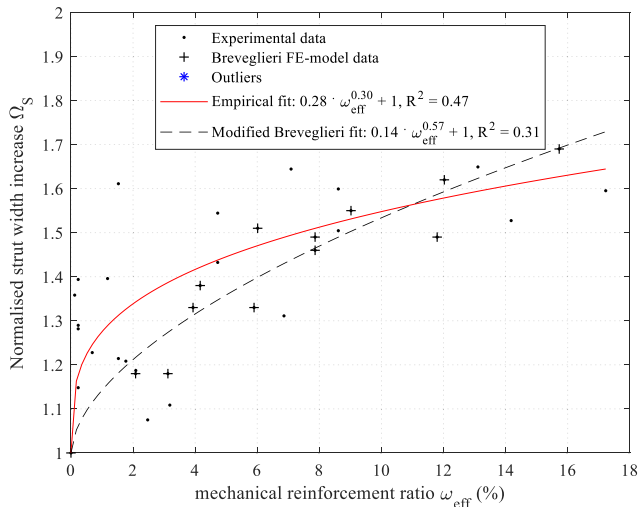


Fig. 5. Increase in secant stiffness against ω_{eff} for the experiments on composite strengthened frames.

the data points obtained from FE-modelling very well, however, the fit with the experimentally obtained values is poor ($R^2 = 0.31$). Instead a new empirical equation is proposed for the strut width increase ($\Omega_{s,emp}$) based on the experimental data alone:

$$\Omega_{s,emp} = 0.28 \cdot \omega_{eff}^{0.30} + 1 (R^2 = 0.47) \quad (16)$$

The empirical fit equation is obtained by least square fitting excluding outliers. Outliers are defined based on a difference of 1.65 times the standard deviation based on the model, i.e. corresponding to a 90% confidence interval. One outlier is considered in this case. The obtained empirical fit is less good than the initial one obtained by Breveglieri et al. [44]. However, it includes a larger range of mechanical strengthening ratios and is based on a range of different experiments. The reasons for the low R^2 -value (0.47) may be related to the stiffness of the retrofitted frames being affected significantly by potential pre-damage in the frames, by the different types of anchorage used, as well as by the application of composite retrofit (full-face or diagonal strip), i.e. factors that cannot be considered in the empirical equation. The issue of obtaining an adequate model for the stiffness of composite retrofitted infilled frames echoes previous findings by Akin et al. [55] on FRP strengthened frames.

4.4. Empirical tie strength equation

A quasi-linear empirical equation of the normalised tie strength is proposed in this section. The normalised tie strength is expressed in relation to the effective mechanical ratio (ω_{eff}), similarly to the calibrated strut width increase Eq. (14). The proposed equation is obtained by least square fitting excluding the outliers defined based on a difference of 1.65 times the standard deviation based on the model, i.e. corresponding to a 90% confidence interval.

$$\Omega_{tie} = 0.19 \cdot \omega_{eff}^{0.98} (R^2=0.96) \quad (17)$$

For the sake of completeness, Fig. 6 displays the experimental data gathered from the experiments in Table 2, highlighting the outliers, and the empirical fit equation considering said outliers. The goodness of fit for the equation is very high, however further empirical data, particularly for higher mechanical reinforcement ratios is still needed for a more adequate equation. Moreover, a majority of the experimental data is coming from scaled specimens, which can have a non-proportional effect on retrofit effectiveness [21,68].

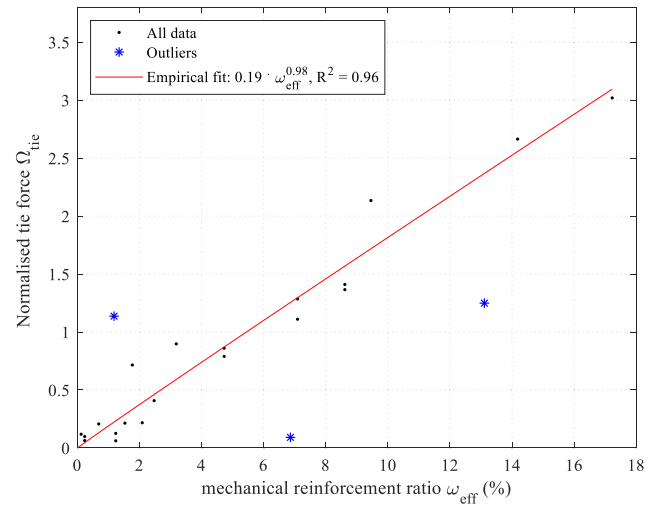


Fig. 6. Normalised tie force against ω_{eff} for the experiments on composite strengthened frames.

5. Analysis and discussion

In this Section, the derived empirical strut-and-tie model equations are analysed and a discussion on their adequacy and limitations is provided. Finally, a simplified retrofit design methodology is proposed.

5.1. Quantitative analysis of the proposed empirical model

First, the assumption of effective tie width in the diagonal, $w_{eff,\theta}$, being equal to 25% of the diagonal length can be evaluated by looking at the obtained agreement for the fitting equations. Table 4 shows the R^2 -values for the fitting equations obtained with different values of $w_{eff,\theta}$. The highest R^2 -value is indeed obtained with $w_{eff,\theta} = 0.25 d_m$, indicating that the chosen effective width definition correlates well with the experimental data. However, high coefficients of determination for values of $w_{eff,\theta} = 0.167$ or $0.2 d_m$ indicate that other assumptions for $w_{eff,\theta}$ may also render adequate empirical equations.

To further assess the adequacy of the model, it is verified that the equation of tie strength does not lead to physically inadequate results, the effective strain ϵ_{eff} in the strengthening material is calculated for all strengthened specimens. In Fig. 7 the obtained values of ϵ_{eff} are plotted against the mechanical strengthening ratio and the respective normalised tie force (Ω_{tie}). As can be seen, the effective strain obtained for the calculated tie forces broadly take values up to 0.45%, and hence takes similar values to the models proposed previously [16,54] and, more crucially, it is well below the maximum FRP or TRM fracture strain.

While it is out of scope for this macro-model to define the failure mode of the composites (e.g. debonding, fibre rupture etc.), effective strain in the tie is generally below 0.3%, indicating that debonding of the composite might occur locally (as it was observed in some of the

Table 4
 R^2 -values for different effective tie width factors in terms of the infill diagonal.

$w_{eff,\theta}$ (% of d_m)	R^2
10%	0.81
13.3%	0.81
16.7%	0.92
20%	0.94
25%	0.96
33.3%	0.87
50%	0.84

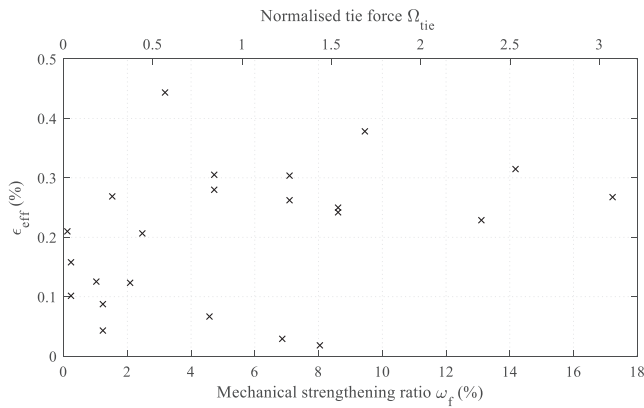


Fig. 7. Effective strain in the composite obtained for the calculated normalised tie force.

experiments), without however being the critical failure mode. The occurrence of debonding, fibre rupture etc.) depend on the presence and effectiveness of anchorage, which is also out of the scope of the macro-model.

To assess the estimation error of the empirical equations for the secant stiffness and the maximum base shear of the retrofitted specimens, an analysis for all specimens from Table 2 was carried out. Fig. 8 shows the average estimation error (in %) for secant stiffness and strength using the empirical equations compared to the experimentally obtained values, separated for TRM and FRP-retrofitted specimens. As can be seen, the secant stiffness is generally underestimated by 13.1% on average for FRP specimens, and 3.7% for TRM specimens.

The standard error is also shown to highlight the variability in the estimation. In both cases a large standard error indicates a large dispersion of the estimated results. This large dispersion may stem from the geometry of the retrofit application (i.e. a diagonal strip application may not increase the stiffness of the infill as much as a full-face application) or the use of different types of anchorage systems, which are difficult to quantify in an empirical equation. The larger standard error for the TRM specimens (18.9%) indicates that the difference between FRP and TRM application (i.e. epoxy vs. mortar) also plays a role in the reliability of the model.

On the other hand, the estimation of the maximum lateral force increase, i.e. taking into account the total strength increase due to the increased strut width and the tie, shows an average estimation error close to zero (1.2% and 0.1% for FRP and TRM, respectively). The

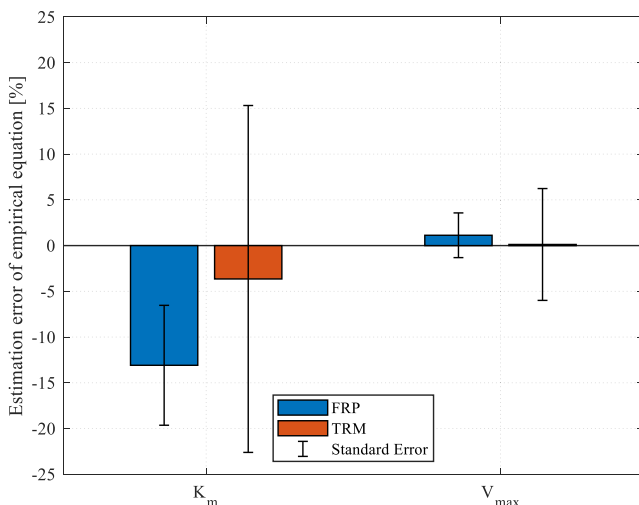


Fig. 8. Estimation error of empirical equation for secant stiffness (K_m) and maximum lateral load capacity increase (V_{max}).

standard error is again higher for the TRM specimens (6.1%). This analysis highlights that the equations for the proposed strut-and-tie model for composite retrofitted infilled frames estimate the strength increase adequately, while the increase in stiffness is generally underestimated. While the estimation error is different for TRM and FRP specimens, using the larger combined dataset is still justified at this stage, but it may be worth investigating separate empirical fitting equations when more experimental data for FRP and TRM strengthened infilled frames will be available.

5.2. Qualitative interpretation of damage using the proposed model

The proposed model allows for an interesting analysis of the relative contribution from the tensile tie (V_{tie}) and the increased compressive strut contribution (ΔV_{strut}) to the total strength increase ($\Delta V = V_{tie} + \Delta V_{strut}$). The total strength increase split into the contribution of the tie and strut, calculated with the proposed model is shown in Fig. 9. This allows a qualitative comparison to be made with the observed damage or failure of the experimental specimens, with respect to compressive and tensile mechanisms associated to the strut and tie, respectively. The empirical equations refer to the peak parameters (strength and stiffness at peak) for the strengthened specimens. Correlation with observed damage is hence attributed to the damage mechanism related to the main lateral load resisting mechanism in the infill.

Table 5 illustrates experimental damage in specimens selected indicatively from the experimental database. For instance, looking at the results for the experiment by Koutas et al. [31], the compressive contribution due to the increased strut width calculated with the proposed model is one of the highest across all specimens, with over 60% of the total strength increase stemming from the strut. It is interesting to observe that, indeed next to shear sliding cracking and local rupture of the textiles, also significant crushing damage was observed at the end of the test after removal of the TRM jacket. On the other hand, for the specimens strengthened with FRP by Altin et al. [19], the proposed model is dominated by the tensile tie, with up to 80% of the strength increase due to the tensile force. This again replicates well the experimental observations, as rupture of the FRP sheets or FRP anchors was observed at peak loading. Similarly, for the specimen tested by Selim et al. [32], extensive diagonal cracking was observed on the TRM surface, without observation of compressive damage to the bricks, which shows that the tensile tie is strongly activated. This is in line with the model prediction, which shows that approximately 70% of the strength increase is associated to tensile tie. It is worth noting that this analysis is rather

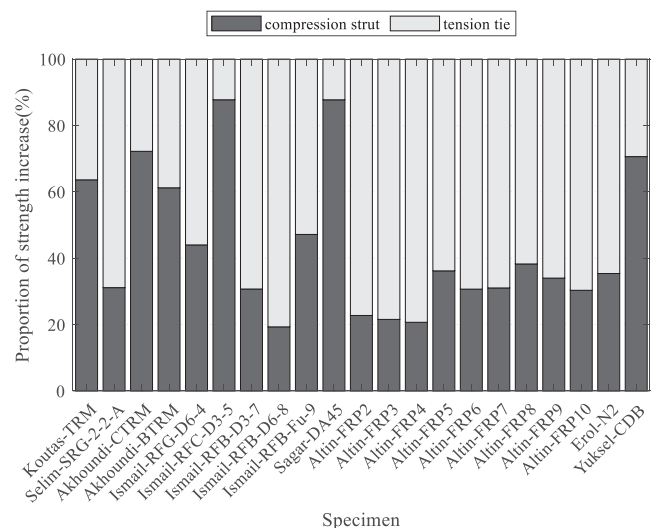


Fig. 9. Relative proportion of total strength increase due to the tie and strut.

Table 5
Summary of observed experimental damage in selected specimens.

Study	Observed damage
Koutas [31]	
Altin et al. [19]	
Selim [32]	

Note:
 cracks
 buckling
 crushed or spalled bricks
 crushed bricks (underneath retrofit material)
 (partial) debonding
 (partial) rupture

qualitative and does not intent to predict the experimental behaviour; instead it compares the split into the tie and strut contributions calculated using the proposed equations with the experimentally observed damage.

5.3. Methodology for simplified retrofit design

As an example for how to use the equations developed herein for the design of retrofitted infilled frames, a design flow-chart highlighting the necessary parameters and equations is provided in Fig. 10. Using the obtained equations for the strut width increase and additional tie force at peak, the total increase in horizontal base shear and stiffness for a specific infill can be determined by combining Eqs. (16) and (17) and (13), respectively:

$$\Delta V = (\Omega_{tie} + \Omega_{s,emp} - 1) \cdot V_{strut,c} \tag{18}$$

$$\Delta K_m = (\Omega_{s,emp} - 1) \cdot K_{m,c} \tag{19}$$

Using the proposed empirical equations, the ratio of calculated strength due to the combined strut and tie strength increases against the experimental base shear is shown in Fig. 11. As expected, the mean value of the ratio is very close to unity (1.01), however the standard deviation is relatively large (0.16). To ensure a safe conservative design, a safety factor is hence proposed based on 1.65 standard deviations of the results (i.e. 90% confidence interval). The obtained multiplication safety factor is 0.74, which ensures 90% of predicted values fall on the conservative side, illustrated in Fig. 11.

In Fig. 12 the total base shear and secant stiffness increase from strut and tie strength increase are plotted against realistic mechanical reinforcement ratios for real-scale infill walls. The curve for strength increase is also shown with the safety factor applied and may be a potential tool for initial design. In terms of the stiffness increase, the use of a safety-factor in design would not be appropriate, as a lower lateral stiffness can lead to an underestimation of the seismic demand. Indicatively, the increase in stiffness against the mechanical reinforcement ratio is still presented in Fig. 12.

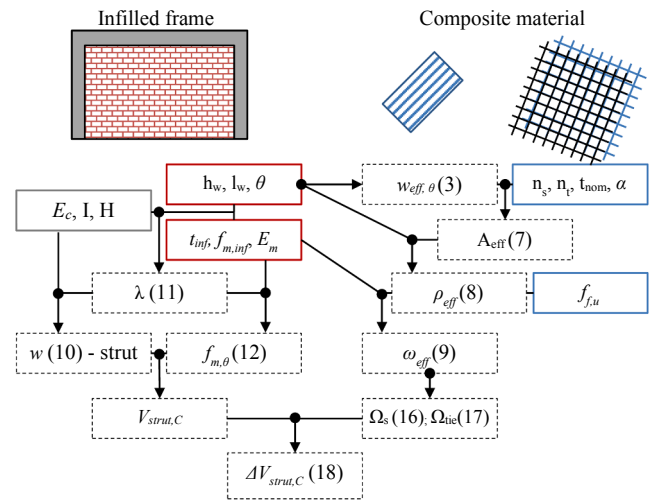


Fig. 10. Design or evaluation flow-chart for composite-strengthened infilled RC frames.

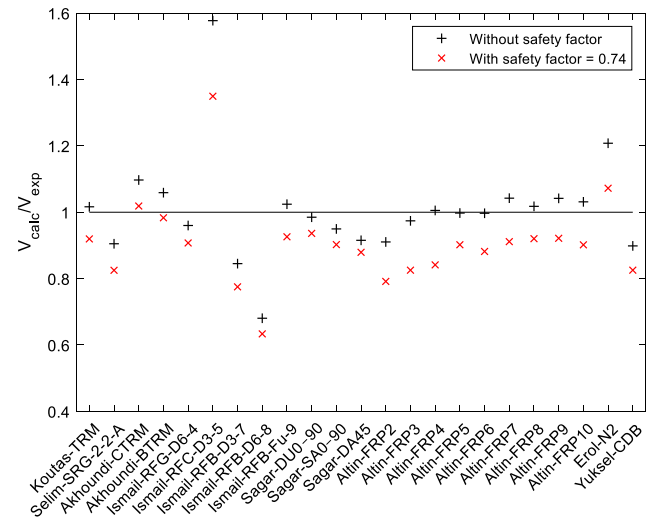


Fig. 11. Ratio of calculated and experimental base shear for all specimens (including outliers).

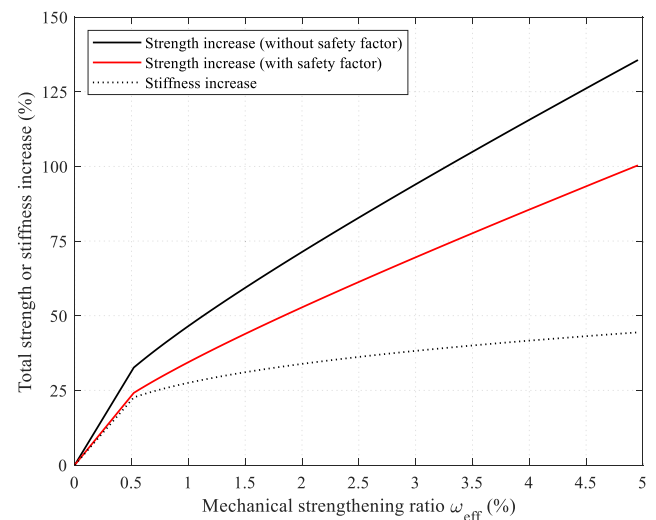


Fig. 12. Design diagram for total base shear and secant stiffness increase against mechanical reinforcement ratio ω_{eff} .

6. Conclusions

A study on a unified design-oriented macro-modelling approach for masonry-infilled RC frames retrofitted with composite materials was presented. It was shown that a variety of materials and layouts have been tested experimentally and yielded satisfactory strengthening results. Damage to the infills can be reduced significantly and larger lateral forces can be sustained. In terms of modelling the retrofitted infills, a new expression for compressive strut width increase due to a better connection between frame and infill was proposed and applied together with a tensile tie.

Using a database of experimental results gathered for this study, empirical equations for the strut and tie model were determined. First, an empirical equation was proposed for the strut width increase based on the increase in secant stiffness for experimentally tested specimens. Based on this new strut width equation, a tensile tie was defined based on the remaining strength increase for the experimental specimens. The equations for normalised strut and tie strength were defined in terms of the effective mechanical reinforcement ratio. The proposed model was found to reproduce experimental findings well in terms of the increase in strength. For the empirical equations relating to the stiffness of retrofitted infills, however, the fit was significantly worse.

Finally, to assist design or evaluation of retrofit schemes, a flow-chart highlighting the required parameters and empirical equations is provided. The presented work gives a promising avenue for design-oriented macro-modelling of strengthened infills, however the present results should be taken with care as there is still need for further experimental data for a wider range of effective geometrical ratios and frame aspect ratios. Experimental data on strengthened frames that present openings or multi-leaf brick arrangements will also be required to further refine the empirical model, as these parameters could not be covered in this study. Future work is recommended to include experimental testing on full-scale masonry-infilled RC frames (control and retrofitted with composites), as well as attempts towards the development of detailed finite-element modelling.

CRedit authorship contribution statement

D.A. Pohoryles: Conceptualization, Methodology, Formal analysis, Software, Validation, Visualization, Writing - original draft. **D.A. Bourmas:** Conceptualization, Writing - review & editing, Supervision, Funding acquisition.

Declaration of Competing Interest

The authors declare that they have no known competing financial interests or personal relationships that could have appeared to influence the work reported in this paper.

Acknowledgements

The work of this study was carried out under the European Commission, Joint Research Centre (JRC) Exploratory Research project **iRESIST+** (Innovative seismic and energy retrofitting of the existing building stock).

References

- [1] Kappos A, Penelis GG. *Earthquake resistant concrete structures*. London/New York: CRC Press; 1996.
- [2] Fikri R, Dizhur D, Walsh K, Ingham J. Seismic performance of reinforced concrete frame with masonry infill buildings in the 2010/2011 Canterbury, New Zealand earthquakes. *Bull Earthq Eng* 2018. <https://doi.org/10.1007/s10518-018-0476-8>.
- [3] Kouris LA, Borg RP, Indirli M. The L'Aquila Earthquake, April 6th, 2009: a review of seismic damage mechanisms. *Proc. Final Conf. COST Action C26 Urban Habitat Constr. Catastrophic Events*, Mazzolani, FM September; 2010, p. 16–18.
- [4] Ricci P, De Luca F, Verderame GM. 6th April 2009 L'Aquila earthquake, Italy: reinforced concrete building performance. *Bull Earthq Eng* 2011;9:285–305.
- [5] Calvi GM, Bolognini D. Seismic response of reinforced concrete frames infilled with weakly reinforced masonry panels. *J Earthq Eng* 2001;05:153–85. <https://doi.org/10.1142/S136324690100039X>.
- [6] Furtado A, Rodrigues H, Arède A, Varum H. Double-leaf infill masonry walls cyclic in-plane behaviour: experimental and numerical investigation. *Open Constr Build Technol J* 2018;12:35–48. <https://doi.org/10.2174/1874836801812010035>.
- [7] Mehrabi AB, Benson Shing P, Schuller MP, Noland JL. Experimental evaluation of masonry-infilled RC frames. *J Struct Eng* 1996;122:228–37. [https://doi.org/10.1061/\(ASCE\)0733-9445\(1996\)122:3\(228\)](https://doi.org/10.1061/(ASCE)0733-9445(1996)122:3(228)).
- [8] Morfidis K, Kostinakis K. The role of masonry infills on the damage response of R/C buildings subjected to seismic sequences. *Eng Struct* 2017;131:459–76. <https://doi.org/10.1016/j.engstruct.2016.10.039>.
- [9] Butenweg C, Marinković M, Salatić R. Experimental results of reinforced concrete frames with masonry infills under combined quasi-static in-plane and out-of-plane seismic loading. *Bull Earthq Eng* 2019;17:3397–422. <https://doi.org/10.1007/s10518-019-00602-7>.
- [10] Furtado A, Rodrigues H, Arède A, Varum H. Simplified macro-model for infill masonry walls considering the out-of-plane behaviour: Macro-model for infill walls considering the out-of-plane behaviour. *Earthq Eng Struct Dyn* 2016;45:507–24. <https://doi.org/10.1002/eqe.2663>.
- [11] Cavaleri L, Zizzo M, Asteris PG. Residual out-of-plane capacity of infills damaged by in-plane cyclic loads. *109957 Eng Struct* 2020;209. <https://doi.org/10.1016/j.engstruct.2019.109957>.
- [12] Di Trapani F, Shing PB, Cavaleri L. Macroelement model for in-plane and out-of-plane responses of masonry infills in frame structures. *J Struct Eng* 2018;144:04017198. [https://doi.org/10.1061/\(ASCE\)ST.1943-541X.0001926](https://doi.org/10.1061/(ASCE)ST.1943-541X.0001926).
- [13] Furtado A, Rodrigues H, Arède A, Varum H. Experimental characterization of the in-plane and out-of-plane behaviour of infill masonry walls. *Procedia Eng* 2015;114:862–9. <https://doi.org/10.1016/j.proeng.2015.08.041>.
- [14] De Luca F, Verderame GM, Gómez-Martínez F, Pérez-García A. The structural role played by masonry infills on RC building performances after the 2011 Lorca, Spain, earthquake. *Bull Earthq Eng* 2014;12:1999–2026. <https://doi.org/10.1007/s10518-013-9500-1>.
- [15] European Commission. The European Green Deal - Communication From The Commission To The European Parliament, The European Council, The Council, The European Economic And Social Committee And The Committee Of The Regions. Brussels: European Commission; 2019.
- [16] Erol G, Karadogan HF. Seismic strengthening of infilled reinforced concrete frames by CFRP. *Compos Part B Eng* 2016;91:473–91. <https://doi.org/10.1016/j.compositesb.2016.01.025>.
- [17] Yuksel E, Ozkaynak H, Buyukozturk O, Yalcin C, Dindar AA, Surmeli M, et al. Performance of alternative CFRP retrofitting schemes used in infilled RC frames. *Constr Build Mater* 2010;24:596–609. <https://doi.org/10.1016/j.conbuildmat.2009.09.005>.
- [18] Ozkaynak H, Yuksel E, Buyukozturk O, Yalcin C, Dindar AA. Quasi-static and pseudo-dynamic testing of infilled RC frames retrofitted with CFRP material. *Compos Part B Eng* 2011;42:238–63. <https://doi.org/10.1016/j.compositesb.2010.11.008>.
- [19] Altin S, Anil Ö, Kara ME, Kaya M. An experimental study on strengthening of masonry infilled RC frames using diagonal CFRP strips. *Compos Part B Eng* 2008;39:680–93. <https://doi.org/10.1016/j.compositesb.2007.06.001>.
- [20] Almusallam TH, Al-Salloum YA. Behavior of FRP strengthened infill walls under in-plane seismic loading. *J Compos Constr* 2007;11:308–18. [https://doi.org/10.1061/\(ASCE\)1090-0268\(2007\)11:3\(308\)](https://doi.org/10.1061/(ASCE)1090-0268(2007)11:3(308)).
- [21] Pohoryles DA, Melo J, Rossetto T, Varum H, Bisby L. Seismic retrofit schemes with FRP for deficient RC beam-column joints: state-of-the-art review. *J Compos Constr* 2019;23:03119001. [https://doi.org/10.1061/\(ASCE\)CC.1943-5614.0000950](https://doi.org/10.1061/(ASCE)CC.1943-5614.0000950).
- [22] Pohoryles DA, Melo J, Rossetto T, D'Ayala D, Varum H. Experimental comparison of novel CFRP retrofit schemes for realistic full-scale RC beam-column joints. *J Compos Constr* 2018;22:04018027. [https://doi.org/10.1061/\(ASCE\)CC.1943-5614.0000865](https://doi.org/10.1061/(ASCE)CC.1943-5614.0000865).
- [23] Koutas LN, Tetta Z, Bourmas DA, Triantafillou TC. Strengthening of concrete structures with textile reinforced mortars: state-of-the-art review. *J Compos Constr* 2019;23:03118001. [https://doi.org/10.1061/\(ASCE\)CC.1943-5614.0000882](https://doi.org/10.1061/(ASCE)CC.1943-5614.0000882).
- [24] Kouris LAS, Triantafillou TC. State-of-the-art on strengthening of masonry structures with textile reinforced mortar (TRM). *Constr Build Mater* 2018;188:1221–33. <https://doi.org/10.1016/j.conbuildmat.2018.08.039>.
- [25] Kapsalis P, El Kadi M, Vervloet J, De Munck M, Wastiels J, Triantafillou T, et al. Thermomechanical behavior of textile reinforced cementitious composites subjected to fire. *Appl Sci* 2019;9:747. <https://doi.org/10.3390/app9040747>.
- [26] Triantafillou TC, Karlos K, Kefalou K, Argyropoulou E. An innovative structural and energy retrofitting system for URM walls using textile reinforced mortars combined with thermal insulation: Mechanical and fire behavior. *Constr Build Mater* 2017;133:1–13. <https://doi.org/10.1016/j.conbuildmat.2016.12.032>.
- [27] Tetta ZC, Bourmas DA. TRM vs FRP jacketing in shear strengthening of concrete members subjected to high temperatures. *Compos Part B Eng* 2016;106:190–205. <https://doi.org/10.1016/j.compositesb.2016.09.026>.
- [28] Raouf SM, Bourmas DA. TRM versus FRP in flexural strengthening of RC beams: Behaviour at high temperatures. *Constr Build Mater* 2017;154:424–37. <https://doi.org/10.1016/j.conbuildmat.2017.07.195>.
- [29] Raouf SM, Bourmas DA. Bond between TRM versus FRP composites and concrete at high temperatures. *Compos Part B Eng* 2017;127:150–65. <https://doi.org/10.1016/j.compositesb.2017.05.064>.
- [30] Cerniauskas G, Tetta Z, Bourmas DA, Bisby LA. Concrete confinement with TRM versus FRP jackets at elevated temperatures. *Mater Struct* 2020;53:58. <https://doi.org/10.1016/j.mater.2020.05.011>.

- [org/10.1617/s11527-020-01492-x](https://doi.org/10.1617/s11527-020-01492-x).
- [31] Koutas L, Bousias S, Triantafillou T. Seismic strengthening of masonry-infilled RC frames with TRM: experimental study. *J Compos Constr* 2015;19:04014048. [https://doi.org/10.1061/\(ASCE\)CC.1943-5614.0000507](https://doi.org/10.1061/(ASCE)CC.1943-5614.0000507).
- [32] Selim M, Okten C, Ozkan M, Gencoglu . Behavior of RC Frames with Infill Walls Strengthened by Cement Based Composites, International Society of Offshore and Polar Engineers; 2015.
- [33] Akhouni F, Vasconcelos G, Lourenço P, Vasconcelos G, Lourenço P. In-plane behavior of infills using glass fiber shear connectors in textile reinforced mortar (TRM) technique. *Int J Struct Glass Adv Mater Res* 2018;2:1–14. <https://doi.org/10.3844/sgamrsp.2018.1.14>.
- [34] Akhouni F, Vasconcelos G, Lourenço P, Silva LM, Cunha F, Fangueiro R. In-plane behavior of cavity masonry infills and strengthening with textile reinforced mortar. *Eng Struct* 2018;156:145–60. <https://doi.org/10.1016/j.engstruct.2017.11.002>.
- [35] Ismail N, El-Maaddawy T, Khattak N. Quasi-static in-plane testing of FRCM strengthened non-ductile reinforced concrete frames with masonry infills. *Constr Build Mater* 2018;186:1286–98. <https://doi.org/10.1016/j.conbuildmat.2018.07.230>.
- [36] Sagar SL, Singhal V, Rai DC. In-plane and out-of-plane behavior of masonry-infilled RC frames strengthened with fabric-reinforced cementitious matrix. *J Compos Constr* 2019;23:04018073. [https://doi.org/10.1061/\(ASCE\)CC.1943-5614.0000905](https://doi.org/10.1061/(ASCE)CC.1943-5614.0000905).
- [37] da Porto F, Guidi G, Verlatto N, Modena C. Effectiveness of plasters and textile reinforced mortars for strengthening clay masonry infill walls subjected to combined in-plane/out-of-plane actions / Wirksamkeit von Putz und textiltbewehrtem Mörtel bei der Verstärkung von Ausfachungswänden aus Ziegelmauerwerk, die kombinierter Scheiben- und Plattenbeanspruchung ausgesetzt sind. *Mauerwerk* 2015;19:334–54. <https://doi.org/10.1002/dama.201500673>.
- [38] Gkourmelos PD, Triantafillou TC, Bournas DA. Structural and Energy Retrofitting of Masonry Walls: The Effect of In-plane Damage on the Out-of-plane Response. *J Compos Constr* n.d. [https://doi.org/10.1061/\(ASCE\)CC.1943-5614.0001066](https://doi.org/10.1061/(ASCE)CC.1943-5614.0001066).
- [39] Koutas LN, Bournas DA. Out-of-plane strengthening of masonry-infilled RC frames with textile-reinforced mortar jackets. *J Compos Constr* 2019;23:04018079. [https://doi.org/10.1061/\(ASCE\)CC.1943-5614.0000911](https://doi.org/10.1061/(ASCE)CC.1943-5614.0000911).
- [40] Gkourmelos PD, Bournas DA, Triantafillou TC. Combined seismic and energy upgrading of existing reinforced concrete buildings using TRM jacketing and thermal insulation. *Earthq Struct* 2019;16:625–39. <https://doi.org/10.12989/EAS.2019.16.5.625>.
- [41] Bournas DA. Concurrent seismic and energy retrofitting of RC and masonry building envelopes using inorganic textile-based composites combined with insulation materials: A new concept. *Compos Part B Eng* 2018;148:166–79. <https://doi.org/10.1016/j.compositesb.2018.04.002>.
- [42] Pohoryles DA, Maduta C, Bournas DA, Kouris LA. Energy performance of existing residential buildings in Europe: A novel approach combining energy with seismic retrofitting. *110024 Energy Build* 2020;223. <https://doi.org/10.1016/j.enbuild.2020.110024>.
- [43] Asteris PG, Antoniou ST, Sophianopoulos DS, Chrysostomou CZ. Mathematical macromodeling of infilled frames: state of the art. *J Struct Eng* 2011;137:1508–17. [https://doi.org/10.1061/\(ASCE\)ST.1943-541X.0000384](https://doi.org/10.1061/(ASCE)ST.1943-541X.0000384).
- [44] Breveglieri M, Camata G, Spacone E. Strengthened infilled RC frames: Continuum and macro modeling in nonlinear finite element analysis. *Compos Part B Eng* 2018;151:78–91. <https://doi.org/10.1016/j.compositesb.2018.05.042>.
- [45] Chrysostomou CZ, Asteris PG. On the in-plane properties and capacities of infilled frames. *Eng Struct* 2012;41:385–402. <https://doi.org/10.1016/j.engstruct.2012.03.057>.
- [46] Crisafulli FJ, Carr AJ, Park R. Analytical modelling of infilled frame structures—a general review. *Bull-N Z Soc Earthq Eng* 2000;33:30–47.
- [47] Di Trapani F, Macaluso G, Cavaleri L, Papia M. Masonry infills and RC frames interaction: literature overview and state of the art of macromodeling approach. *Eur J Environ Civ Eng* 2015;19:1059–95. <https://doi.org/10.1080/19648189.2014.996671>.
- [48] Tanganelli M, Rotunno T, Viti S. On the modelling of infilled RC frames through strut models. *Cogent Eng* 2017;4:1371578. <https://doi.org/10.1080/23311916.2017.1371578>.
- [49] Pantò B, Caliò I, Lourenço PB. Seismic safety evaluation of reinforced concrete masonry infilled frames using macro modelling approach. *Bull Earthq Eng* 2017;15:3871–95. <https://doi.org/10.1007/s10518-017-0120-z>.
- [50] Kareem KM, Pantò B. Simplified macro-modelling strategies for the seismic assessment of non-ductile infilled frames: a critical appraisal. *J Build Eng* 2019;22:397–414.
- [51] Paulay T, Priestley M.J.N. *Seismic design of reinforced concrete and masonry buildings*. 1st ed. New York: Wiley-Interscience; 1992.
- [52] Pardalopoulos SI, Pantazopoulou SJ, Thermou GE. Seismic rehabilitation of sub-standard R.C. buildings with masonry infills. 0:1–30 *J Earthq Eng* 2018. <https://doi.org/10.1080/13632469.2018.1453397>.
- [53] Binici B, Ozebe G, Ozelcik R. Analysis and design of FRP composites for seismic retrofit of infill walls in reinforced concrete frames. *Compos Part B Eng* 2007;38:575–83. <https://doi.org/10.1016/j.compositesb.2006.08.007>.
- [54] Binici B, Ozebe G. Analysis of infilled reinforced concrete frames strengthened with FRPs. In: Wasti ST, Ozebe G, editors. *Adv. Earthq. Eng. Urban Risk Reduct.*, vol. 66, Dordrecht: Kluwer Academic Publishers; 2006, p. 455–70. https://doi.org/10.1007/1-4020-4571-9_30.
- [55] Akin E, Özebe G, Canbay E, Binici B. Numerical study on CFRP strengthening of reinforced concrete frames with masonry infill walls. *J Compos Constr* 2015;19:04013034. [https://doi.org/10.1061/\(ASCE\)CC.1943-5614.0000426](https://doi.org/10.1061/(ASCE)CC.1943-5614.0000426).
- [56] Koutas L, Triantafillou TC, Bousias SN. Analytical modeling of masonry-infilled RC frames retrofitted with textile-reinforced mortar. *J Compos Constr* 2015;19:04014082. [https://doi.org/10.1061/\(ASCE\)CC.1943-5614.0000553](https://doi.org/10.1061/(ASCE)CC.1943-5614.0000553).
- [57] Pohoryles DA, Bournas DA. Seismic retrofit of infilled RC frames with textile reinforced mortars: State-of-the-art review and analytical modelling. *107702 Compos Part B Eng* 2020;183. <https://doi.org/10.1016/j.compositesb.2019.107702>.
- [58] Mainstone RJ. Supplementary note on the stiffness and strength of infilled frames. *Curr Pap CP1374 Build Res Establ Lond* 1974.
- [59] Bertoldi SH, Decanini LD, Gavardini C. Telai tamponati soggetti ad azioni sismiche, un modello semplificato: confronto sperimentale e numerico. *Atti Del* 1993;6:815–24.
- [60] Stafford Smith B, Carter C. A method of analysis for infilled frames. *Proc Inst Civ Eng* 1969;44:31–48. <https://doi.org/10.1680/icep.1969.7290>.
- [61] Asteris PG, Cavaleri L, Trapani FD, Sarhosis V. A macro-modelling approach for the analysis of infilled frame structures considering the effects of openings and vertical loads. *Struct Infrastruct Eng* 2016;12:551–66. <https://doi.org/10.1080/15732479.2015.1030761>.
- [62] Mainstone RJ. On the stiffness and strengths of infilled frames. *Proc Inst Civ Eng* 1971;49:230.
- [63] Perrone D, Leone M, Aiello MA. Non-linear behaviour of masonry infilled RC frames: Influence of masonry mechanical properties. *Eng Struct* 2017;150:875–91. <https://doi.org/10.1016/j.engstruct.2017.08.001>.
- [64] American Concrete Institute, American Society of Civil Engineers, Masonry Society, Masonry Standards Joint Committee. TMS 402-11/ACI 530-11/ASCE 5-11 - Building code requirements and specification for masonry structures. Boulder, Co.; Farmington Hills, Mi.; Reston, Va.: The Masonry Society ; American Concrete Institute ; American Society of Civil Engineers; 2013.
- [65] Decanini LD, Fantin GE. Modelos simplificados de la mampostería incluida en porticos. *Características Stiffness Resist Lateral En Estado Lte Jorn Argent Ing Estructural* 1986;2:817–36.
- [66] Korkmaz SZ, Kamanli M, Korkmaz HH, Donduren MS, Cogurcu MT. Experimental study on the behaviour of nonductile infilled RC frames strengthened with external mesh reinforcement and plaster composite. *Nat Hazards Earth Syst Sci* 2010;10:2305–16. <https://doi.org/10.5194/nhess-10-2305-2010>.
- [67] Altun S, Anil Ö, Koprman Y, Belgin Ç. Strengthening masonry infill walls with reinforced plaster. *Proc Inst Civ Eng - Struct Build* 2010;163:331–42. <https://doi.org/10.1680/stbu.2010.163.5.331>.
- [68] Choudhury AM, Deb SK, Dutta A. Study on size effect of fibre reinforced polymer retrofitted reinforced concrete beam–column connections under cyclic loading. *Can J Civ Eng* 2013;40:353–60. <https://doi.org/10.1139/cjce-2012-0041>.